Dynamic Pd(II) /Cu(I) Multimetallic Assemblies as Molecular Models to Study Metal-Metal Cooperation in Sonogashira Coupling

doi: info:doi/10.1002/chem.202002013

Chemistry
A European
Journal

Chemistry Europe
European Chemical Societies Publishing

Accepted Article

Title: Dynamic PdII/CuI multimetallic assemblies as molecular models to study metal-metal cooperation in Sonogashira coupling

Authors: Orestes Rivada-Wheelaghan, Aleix Comas-Vives, Robert R. Fayzullin, Agustí Lledós, and Julia Khusnutdinova

To be cited as: *Chem. Eur. J.* 10.1002/chem.202002013

Link to VoR: https://doi.org/10.1002/chem.202002013

WILEY-VCH

10.1002/chem.202002013

WILEY-VCH

Dynamic Pd^{II}/Cu^{I} multimetallic assemblies as molecular models to study metal-metal cooperation in Sonogashira coupling

Orestes Rivada-Wheelaghan,[a]† Aleix Comas-Vives,[b] Robert R. Fayzullin,[c] Agustí Lledós,*[b] Julia R. Khusnutdinova*[a]

[a] Dr. O. Rivada-Wheelaghan and Prof. J. R. Khusnutdinova
Coordination Chemistry and Catalysis Unit
Okinawa Institute of Science and Technology Graduate University
1919-1 Tancha, Onna-son, Okinawa, Japan 904-0495
E-mail: juliak@oist.jp
†Current address: Université de Paris, Laboratoire d'Electrochimie Moléculaire, UMR 7591 CNRS, 15 rue Jean-Antoine de Baïf, F-75205, Paris Cedex 13, France
[b] Dr. A. Comas-Vives and Prof. A. Lledós
Departament de Química
Universitat Autònoma de Barcelona
08193 Bellaterra, Barcelona, Catalonia, Spain.
E-mail: agusti@klingon.uab.es
[c] Dr. R. R. Fayzullin
Arbuzov Institute of Organic and Physical Chemistry
FRC Kazan Scientific Center, Russian Academy of Sciences
8 Arbuzov Street, Kazan, 420088, Russian Federation.

Supporting information for this article is given via a link at the end of the document.

10.1002/chem.202002013

Abstract: Cooperation between two different metals plays a crucial role in many synergistic catalytic reactions such as the Sonogashira C-C cross-coupling reaction, where an interaction between the Pd and Cu centers is proposed in the transmetallation step. Although several heterobimetallic Pd/Cu complexes were proposed as structural models of the active species in Sonogashira coupling, the detailed understanding of the metal-metal cooperation in transmetallation is still lacking in current systems. In this work, we report a stepwise and systematic approach to building heteromultimetallic Pd/Cu assemblies as a tool to study metal-metal cooperativity. We obtained fully characterized Pd/Cu multimetallic assemblies that show reactivity in alkyne activation, formation of catalytically relevant aryl/acetylide species, and C-C elimination, serving as functional models for Sonogashira reaction intermediates. The combined experimental and DFT studies highlight the importance of ligand-controlled coordination geometry, metal-metal distances and dynamics of the multimetallic assembly for transmetallation step.

Palladium-catalyzed C-C cross-coupling and the more recently developed combined C-H activation/C-C coupling reactions[1] are among the most powerful and widely used methodologies for synthesizing fine pharmaceuticals, biologically active compounds and precursors for materials chemistry.[2] Due to the significant impact of palladium-catalyzed C-C coupling reactions on the development of synthetic methodologies, the detailed mechanistic understanding of these reactions remains an active area of study.[3] In many cases, d^{10} metal additives are required to assist Pd-catalyzed C-C coupling or C-H functionalization reactions,[1a, 4] and the mechanism of cooperation between the two metals is often poorly understood due to the its high complexity.[5] For example, Sonogashira coupling is a well-known C-C cross-coupling reaction which results in the formation of a new C-C bond between a terminal alkyne and an aryl or vinyl halide, and it generally requires a Pd catalyst in the presence of a Cu^{I} co-catalyst and at least a stoichiometric amount of base (Figure 1, a).[6] The accelerating effect of copper on the rate of Pd-catalyzed C-C coupling reactions is often referred to as the "copper effect", however, the detailed understanding of the underlying mechanism is still lacking.[7] To account for the participation of a Cu^{I} co-catalyst in Sonogashira coupling, the proposed catalytic cycle is usually divided into "palladium cycle" and "copper cycle" (Figure 1, a), with the general mechanism consisting of three major steps: oxidative addition, transmetalation, and reductive elimination.[6] However, a fundamental understanding of the transmetalation step, the merging point for the two separate Pd and Cu-cycles, as well as the structural requirements for the proposed heterobimetallic Pd^{II}/Cu^{I} intermediates,[8] are lacking, due to difficulty of directly isolating such short-lived intermediates. Although bimetallic Pd/Cu species were proposed based on computational studies in a Sonogashira coupling cycle, the absence of directly observed reactivity of such species in alkyne activation and C-C elimination can always raise a question about the direct relevancy of such heterobimetallic complexes in these transformations.[8]

In this context, studying heterobimetallic organometallic species with well-defined structure and metal-metal distances is an active area of research aimed to provide insights into the role of metal-metal cooperation in bond activation. In particular, several important studies appeared describing Pd^{II}/Cu^{I} complexes featuring aryl, vinyl and/or acetylide ligands, which may be considered as structural, even if not as functional models for the transmetalation step.[9] Chen and co-workers recently reported the crystal structure of a bimetallic complex featuring close interactions between bis-aryl Pd^{II} and Cu^{I} centers, and it was proposed as a plausible structural model for the Sonogashira transmetalation step's transition state (Figure 1, b).[9b] In addition, Albéniz and co-workers also reported model acetylide complexes in which both Pd and Cu were present, synthesized from pre-formed Cu-acetylide species.[9a] However, the structurally characterized examples featuring Pd vinyl-acetylide complexes interacting with a copper center did not undergo C(sp)-C(sp^2) bond formation even in the presence of phosphines or other additives known to promote C-C bond elimination.[9a] Overall, there are currently no examples of functional models featuring Pd/Cu^{I} aryl-acetylide complexes formed by the direct activation of a terminal alkyne, which would ultimately lead to C-C bond formation, limiting our current understanding of what role the metal-metal cooperation may play in the Sonogashira coupling and related reactions.

We have recently reported a new modular approach to construct and deconstruct homomultimetallic assemblies using dynamic unsymmetrical ligand scaffolds based on the napthyridinone (Naph) framework.[10] This new approach allowed for the stepwise formation of di-, tri- and tetranuclear Cu^{I} one-dimensional chains controlled by reaction conditions and stoichiometry.[10] In this work we extend this approach to selectively create heteromultimetallic Pd^{II}/Cu^{I} assemblies of variable nuclearity with the aim to isolate and study organometallic complexes relevant to Pd coupling chemistry (i.e. Sonogashira coupling). A noteworthy intermediate, able to undergo selective C(sp)-C(sp^2) bond formation has been characterized, and state-of-the-art static and dynamic DFT calculations have analyzed ligand and metal cooperativity in the coupling pathway. These combined experimental and computational studies also reveal the important role of metal-metal distances for transmetalation step (Figure 1, c). Formation of such modular, dynamic heteromultimetallic complexes is therefore a powerful tool for the detailed study of the mechanism of metal-metal cooperation in fundamental bond breaking and bond formation steps in synergistic, bimetallic catalysis.[5b, 5c, 11] We have also recently demonstrated applications of similar ligand design-driven approach for studying metal-metal cooperativity in bond activation by Pt/Cu organometallic complexes.[12]

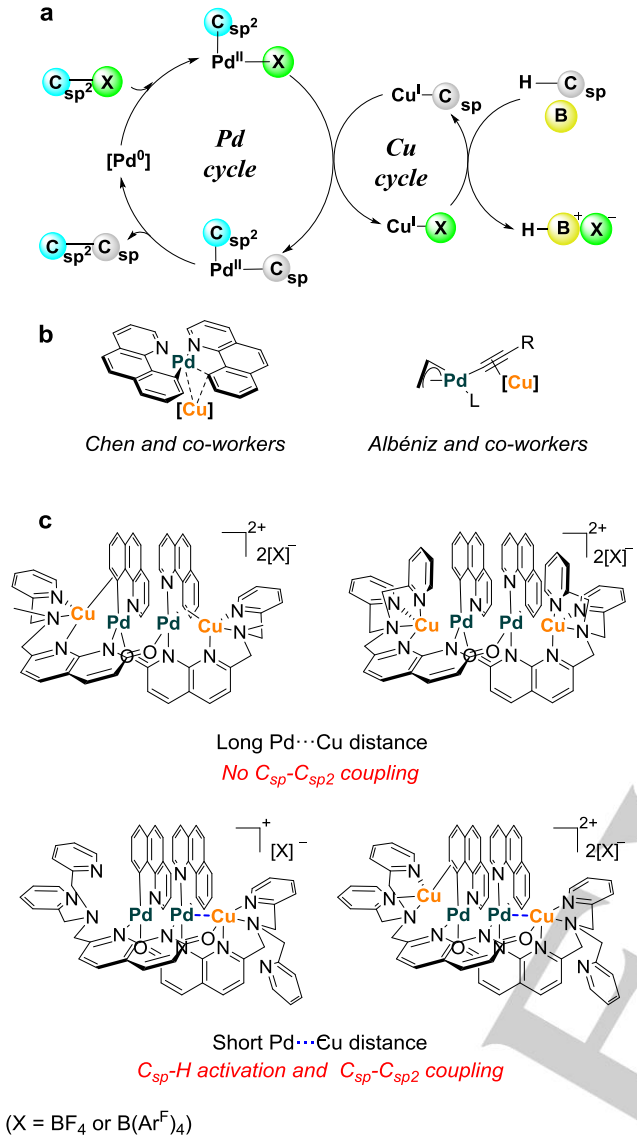

Figure 1. The Pd and Cu complexes and their heteromultimetallic assemblies in Sonogashira coupling: **(a)** General proposed mechanism for Sonogashira cross-coupling reactions. **(b)** Molecular models reported in the literature to study Sonogashira-type cross-coupling. **(c)** Multimetallic chain complexes herein reported as molecular models to study Sonogashira-type cross-coupling reactions.

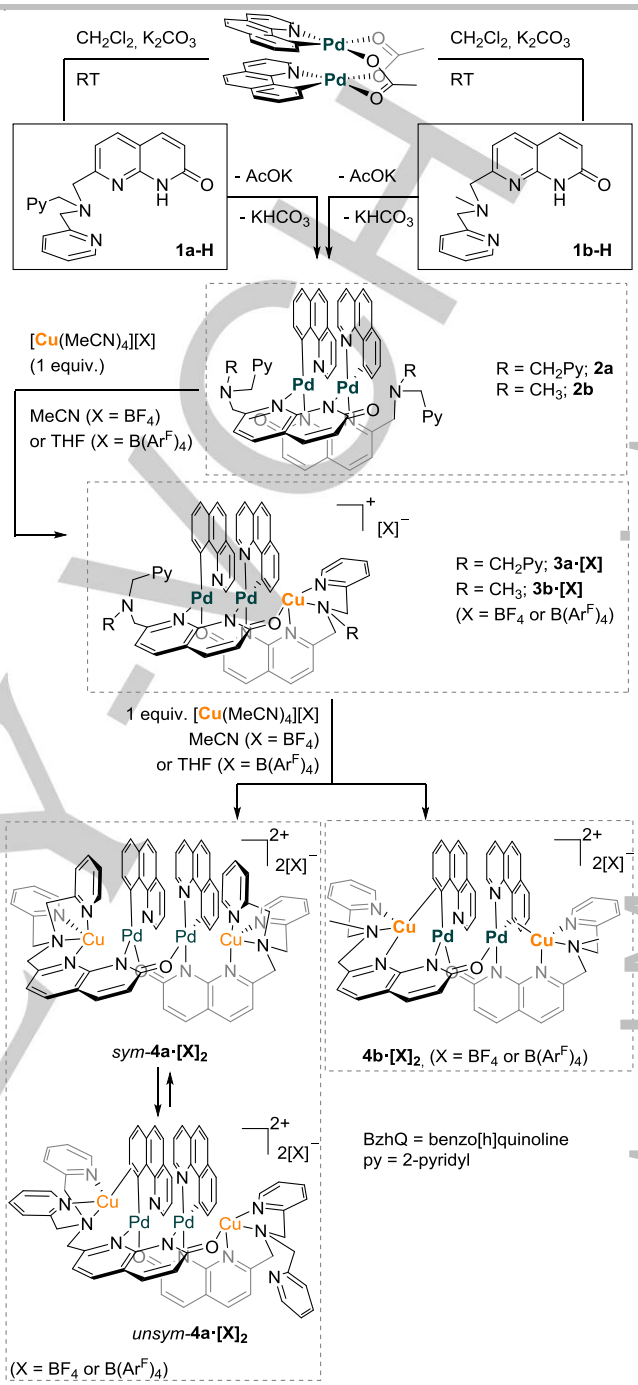

Scheme 1. Formation of the multimetallic linear chain complexes.

Results and Discussion

Stepwise formation of heteromultimetallic Pd^{II}/Cu^{I} complexes. First, we set out to investigate whether we can promote the formation of heteropolymetallic Pd^{II}/Cu^{I} chains based on the previous success with purely Cu based polymetallic chains.

First, substitution of the acetate ligand from the benzo[h]quinoline (BzhQ) palladium dimer, $[Pd(BzhQ)(AcO)]_2$ was achieved by reaction of 2 equiv of neutral ligands, L = **1a-H** or L = **1b-H**, in dichloromethane in the presence of 4 equiv of K_2CO_3 yielding the dinuclear neutral Pd^{II}_2 dimers **2a** and **2b** in 79-89% isolated yields (Scheme 1). The symmetrical pattern observed by NMR spectra in solutions of **2a** and **2b** indicate that the palladium atoms have the same coordination environment. Single crystal X-ray diffraction (XRD)[13] analysis of **2a** and **2b** confirmed their Pd-Pd core binding to two N-atoms of naphthyridinone with the same coordination environment around each Pd center (Figure 2, a). Having pendant picolylamine capping units, we envisioned that this will

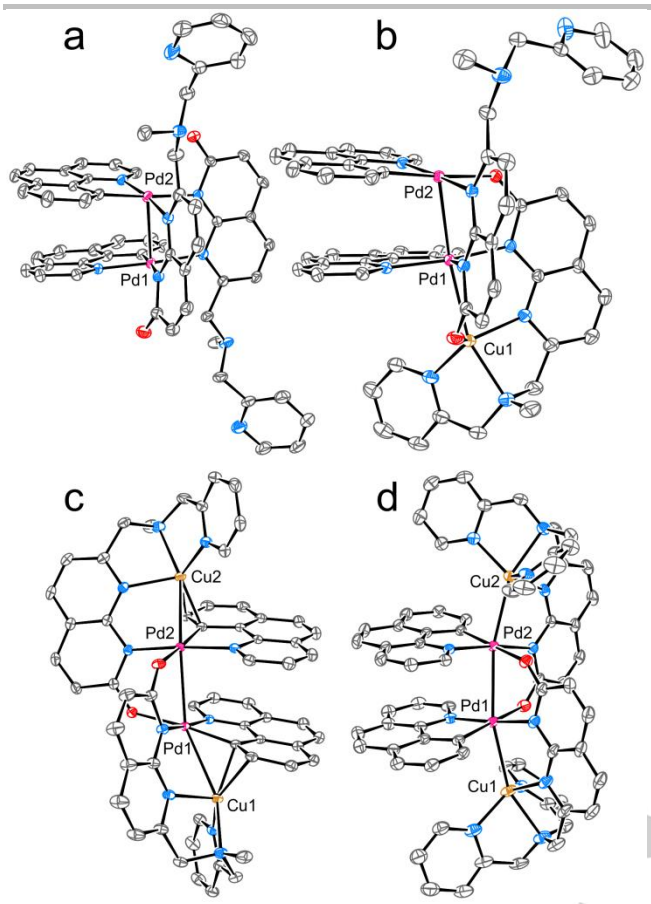

Figure 2. ORTEP of the cationic parts of **2b (a)**, **3b·[B(Ar^F)$_4$] (b)**, **4b·[B(Ar^F)$_4$]$_2$ (c)**, and *sym*-**4a·[B(Ar^F)$_4$]$_2$ (d)** at 50 % probability level according to single crystal X-ray diffraction data. Counterions, hydrogen atoms, minor disordered components, and solvent molecules are omitted for clarity. Hereinafter metal-metal bonds are shown if the interatomic distances are shorter than sum of the corresponding van der Waals radii. The structures of **2a** and **4b·[BF$_4$]$_2$** are shown in the Supporting Information.

enable further metal chain growth, allowing us to introduce a different metal ion.

Accordingly, when 1 equiv of [Cu(MeCN)$_4$][X] (X = BF$_4$ or B(Ar^F)$_4$; B(Ar^F)$_4$ = tetrakis[3,5-bis(trifluoromethyl)phenyl]borate) was added to a solution of **2a** or **2b** in THF (X = B(Ar^F)$_4$) or MeCN (X = BF$_4$), the new unsymmetrical trinuclear monocationic complexes **3a·[X]**, [Pd$_2$Cu(BzhQ)$_2$(**1a**)$_2$][X] and **3b·[X]** [Pd$_2$Cu(BzhQ)$_2$(**1b**)$_2$][X] respectively, were obtained and isolated in 80-90% yields (Scheme 1). The reaction occurred selectively within seconds at 20 °C generating only one major product observed by ^{1}H NMR spectroscopy. The identity of the counter-anion did not affect solution NMR spectra. X-ray structure of **3b·[B(Ar^F)$_4$]** confirmed the linear assembly of two Pd^{II} and one Cu^I atoms (Figure 2b), with a Cu1···Pd1 distance of 2.6727(3) Å, shorter than the sum of van der Waals radii (3.03 Å)[14] and shorter than the sum of covalent radii (2.71 Å).[15] We were unable to obtain crystals suitable for X-ray diffraction studies from complex **3a·[X]**, however a similar structure could be invoked through comparison of the ^{1}H and ^{13}C NMR spectra of **3a-b·[X]** in THF-d_8 and MeCN-d_3.[16] As almost identical chemical shifts for proton resonances of the ligand surrounding the metal core were observed, including the benzoquinolyl, unbound picolyl, and Naph fragments, we propose that complex **3a·[X]** should have a structure similar to **3b·[X]** in solution. While complex **3b·[X]** was stable in solution and in the solid state for more than 2 weeks, complex **3a·[X]** showed limited stability and eventually evolved in solution. After prolonged storage in solution at RT, we observed the appearance of small set of peaks in the ^{1}H NMR spectrum of **3a·[X]**, which indicate the formation of **4a·[X]$_2$**; the solution also became slightly turbid as a consequence of the formation of poorly soluble **2a**. Both unsymmetrical Pd$_2$Cu$_1$ complexes **3a-b·[X]** retain an uncoordinated nitrogen-donor capping unit (*bis*- or *mono*-picolyl), suggesting that further extension of the metal chain may still be possible. As expected, treatment of **3b·[X]** with another equivalent of [Cu(MeCN)$_4$][X] in THF (B(Ar^F)$_4$) or MeCN (X = BF$_4$) quantitatively yielded the new symmetrical tetranuclear dicationic species **4b·[X]$_2$**, [Pd$_2$Cu$_2$(BzhQ)$_2$(**1b**)$_2$][X]$_2$, Scheme 1. Alternatively, the same compound could be synthesized more conveniently by adding 2 equiv of the Cu^I precursor directly to a dinuclear Pd$^{II}_2$ complex **2b**. X-ray quality crystals of **4b·[B(Ar^F)$_4$]$_2$** were obtained by crystallization by hexane diffusion into THF solution at -33 °C. The diffraction analysis revealed a symmetrical, linear tetranuclear Cu^I···Pd^{II}···Pd^{II}···Cu^I core (Figure 2, c). Interestingly, as Cu^I centers in **4b·[X]$_2$** have only three available N-atom mono-picolylamine ligand donors, the coordination is complemented by a π-coordination to the double bond of benzoquinolyl. The Cu^I···C$_{ipso}$ bonds lengths are ca. 2.07 Å, slightly longer than those reported by Chen et al. in a Pd(bis-benzoquinolyl)/Cu^I complex (2.025(4) Å).[9b] The symmetrical structure of **4b·[X]$_2$** is evident from the ^{1}H NMR spectrum both in THF-d_8 and MeCN-d_3 solutions, independent on the counterion, Figures S51-S60). The selectivity of the multimetallic metal assembly is demonstrated by ^{1}H NMR titration experiment of complex **2b** in THF-d_8 solution (Figure 3).

Similarly, when complex **3a·[X]** was reacted with 1 equiv of [Cu(MeCN)$_4$][X] precursor in THF (X = B(Ar^F)$_4$) or MeCN (X = BF$_4$), or by directly reacting the Pd$^{II}_2$ dimer **2a** with 2 equiv of Cu^I precursor, a tetranuclear Pd$^{II}_2$Cu$^I_2$ species **4a·[X]$_2$**, **[**Pd$_2$Cu$_2$(BzhQ)$_2$(**1a**)$_2$][X]$_2$, was obtained. Crystallization of **4a·[B(Ar^F)$_4$]$_2$** by slow diffusion of hexane into a THF/toluene solution at -33 °C shows formation of a symmetrical structure (Figure 2d) with a similar Cu^I···Pd^{II}···Pd^{II}···Cu^I core as in complex **4b·[B(Ar^F)$_4$]$_2$**, with the Cu^I centers coordinated to four N-atoms of bis-picolylamine capping unit and a Naph fragment.

All complexes **2b**, **3b·[X]**, **4b·[X]$_2$** and **4a·[X]$_2$** were isolated in high yield and were characterized by NMR, UV/Vis spectroscopy, elemental analysis, and X-ray diffraction. Electrospray mass-spectrometry (ESI-MS) was also used to confirm the persistence of dinuclear, trinuclear, and tetranuclear species in polar solvents.

The ^{1}H NMR spectrum of **4a·[B(Ar^F)$_4$]$_2$** in THF-d_8 solution at -50 °C shows the presence of one major symmetrical species assigned as *sym*-**4a·[B(Ar^F)$_4$]$_2$,** Scheme 2. However, the ^{1}H NMR spectrum of **4a·[B(Ar^F)$_4$]$_2$** in MeCN-d_3 solution shows the presence of one symmetrical and one unsymmetrical species in similar ratio. Identical NMR spectra (except for the presence of counterion peaks of B(Ar^F)$_4$) was obtained in MeCN-d_3 solution for complex **4a·[BF$_4$]$_2$**, showing the innocent nature of the

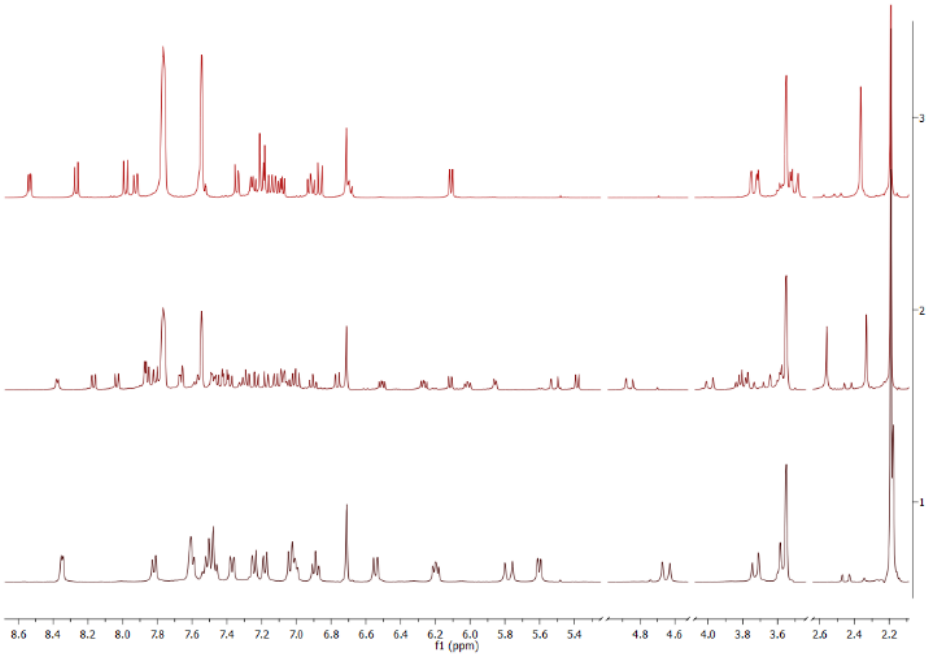

Figure 3. Selective stepwise formation of heteromultimetallic $Pd^{II}Cu^{I}$ assemblies. ^{1}H NMR in THF-d_8 solution at 20 °C: bottom: **2b**; middle: addition of 1 equiv of $[Cu(MeCN)_4][BAr^F]$ to yield **3b·[B(Ar^F)$_4$]**; top: addition of total 2 equiv of $[Cu(MeCN)_4][BAr^F]$ to yield **4b·[B(Ar^F)$_4$]$_2$**.

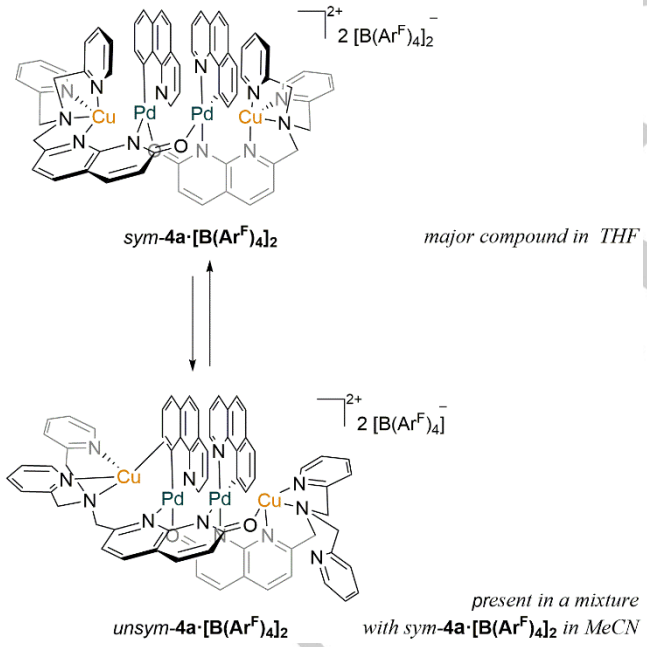

Scheme 2. Reversible isomer interconversion for complex **4a·[B(Ar^F)$_4$]$_2$** in THF and CH_3CN solutions.

counterion.

Interestingly, while complex **4a·[B(Ar^F)$_4$]$_2$** could not be crystallized from MeCN solvent due to its high solubility, **4a·[BF$_4$]$_2$** readily produced crystals from MeCN-containing solutions providing two different isomeric structures whose identity depended on the crystallization conditions. The symmetrical isomer, *sym*-**4a·[BF$_4$]$_2$**, was obtained by slow evaporation of MeCN from a MeCN/toluene mixture at RT and shows a structure similar to that of **4a·[B(Ar^F)$_4$]$_2$** (Figure 4, a). The unsymmetrical isomer, *unsym*-**4a·[BF$_4$]$_2$**, was obtained from a MeCN/THF/diethyl ether mixture at -30 °C and it exhibits different coordination geometries around the two Cu^{I} centers (Figure 4, b). In this structure, one copper ion is surrounded by three N- and one O-donor, while the other copper ion coordinates to three N-donors of the bis-picolylamine and the benzoquinolyl fragment's double bond. In *unsym*-**4a·[BF$_4$]$_2$**, the naphthyridinone framework acts as a trinucleating bridging fragment, similar to **3b·[BF$_4$]** and to the proposed structure of **3a·[BF$_4$]**, where a copper ion binds only through the bis-picolylamine capping unit. Based on these observations, we propose that the two major species observed in the MeCN-d_3 solution of **4a·[BF$_4$]$_2$** likely belong to the symmetrical and unsymmetrical isomers similar to those obtained in the solid state.

The metal-metal bond distances are also affected due to differences in the coordination environment of the two copper ions in *sym*-**4a·[BF$_4$]$_2$** and *unsym*-**4a·[BF$_4$]$_2$**. In particular, there is a significant desymmetrization of $Pd^{II}\cdots Cu^{I}$ distances in *unsym*-**4a·[BF$_4$]$_2$**: the Pd^{II} distance to a Cu^{I} center bound to the O-atom is significantly shorter (Pd1···Cu1 2.6517(3) Å) than the distance between the Pd^{II} and another Cu^{I} center coordinated to the capping unit only on the other side (Pd2···Cu2 3.1820(5) Å); the latter distance resembling the coordination of the Cu^{I} center in **4b·[X]$_2$**. It is also significantly shorter than the $Pd^{II}\cdots Cu^{I}$ distances in *sym*-**4a·[BF$_4$]$_2$** (2.8081(2) and 2.7747(2)

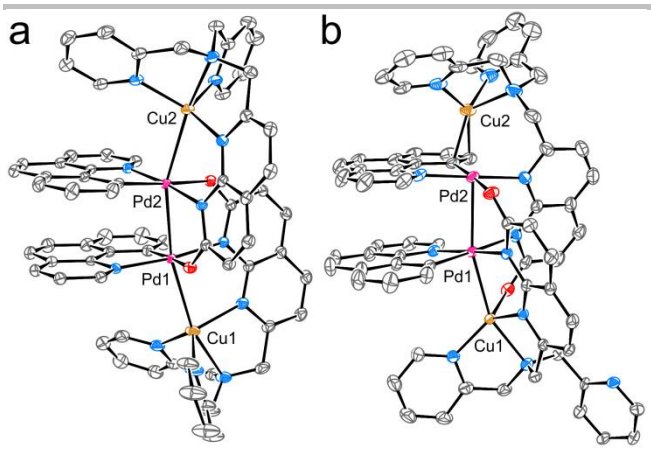

Figure 4. ORTEP of the cationic parts of *sym*-**4a·[BF$_4$]$_2$** (a) and *unsym*-**4a·[BF$_4$]$_2$** (b) at 50 % probability level according to single crystal X-ray diffraction data. Counterions, hydrogen atoms, minor disordered components, and solvent molecules are omitted for clarity.

Å). Such desymmetrization and the presence of a short Pd^{II}···Cu^{I} distance are likely to play an important role in the alkyne activation as confirmed by further experimental and computational studies (vide infra).

Reactivity with a terminal arylacetylene. Considering selective formation and stability of these Pd^{II}(aryl)Cu^{I} polymetallic assemblies in solution, we then decided to use well-defined tetranuclear species, **4a·[X]$_2$** and **4b·[X]$_2$**, as models to study their reactivity with terminal alkynes relevant to the Sonogashira coupling transmetalation step.

Complex **4a·[BF$_4$]$_2$** reacts with 2.2 equiv of 4-ethynylanisole in MeCN solution to a new product within 3h at room temperature (Scheme 3a). This product was structurally characterized by X-ray diffraction as the dinuclear Pd^{II}/Cu^{I} acetylide complex **5a·[BF$_4$]** and was isolated in 73% yield (Figure 5, a). This is a rare example of a Pd^{II}/Cu^{I} complex containing both aryl and acetilyde ligands. Previously related examples ([POCOP]Pd(acetylide)/Au and PdMe(acetylide)/Cu complexes) were reported by R. J. Oeschger and P. Chen.[17] In this structure, the Pd^{II} has been displaced from its original position at the Naph platform and coordinates only to a pyridine arm of bis-picolylamine. Interestingly, the N atom from the Naph fragment is protonated, thus acting as an acceptor of the proton initially residing at the terminal acetylene carbon (Scheme 3, a). The naphthyridinone ligand thus also acts as an internal base participating in alkyne activation (vide infra), resembling the role of the external base in proposed catalytic cycles for Sonogashira coupling (Figure 1, a). The aryl and acetylide ligands are located at *cis*-positions to each other, with the triple bond of the acetylene involved in a π-interaction with the closely located Cu^{I} center. This structure resembles the generally proposed species undergoing reductive elimination in cross-coupling reactions catalyzed by palladium.[8] The new aryl/acetylide complex [PdCu(BzhQ)(MeOPhCC)(**1a**-H)][BF$_4$], **5a·[BF$_4$]**, is stable in the solid state and in solution at temperatures below -15 °C. ^{1}H NMR spectrum measured in MeCN-d_3 exhibits the N-H peak as a broad singlet at 11 ppm. The Pd^{II}-C(*sp*) carbon appears as a singlet in the ^{13}C{^{1}H} spectrum at 103.7 ppm, while the C(*sp*) attached to the aryl fragment appears at 101.1 ppm. These values did not vary significantly with a different counterion or when the NMR spectrum of complex **5a·[B(Ar^{F})$_4$]** was recorded at -15 °C in THF-d_8 solution, suggesting that the Cu^{I} center likely retains its π-interaction with the triple bond in both (potentially coordinating) polar and non-polar solvents.

Surprisingly, when complex **4b·[X]$_2$** was mixed with 4-ethynylanisole, no reaction occurred in various solvents and at temperatures up to 80 °C, and complex **4b·[X]$_2$** remained unchanged. This suggests that even fine changes in copper coordination environment can significantly affect the reactivity. To gain more insight into the reactivity of various Pd^{II}Cu^{I} and Pd^{II}-only species, we then reacted tri-nuclear **3a·[X]** and **3b·[X]** and simple Pd^{II} dimers, **2a** and **2b**, with 4-ethynylanisole under analogous conditions. None of the Pd^{II} dimers **2a** or **2b** gave the desired reactivity with alkynes, and ^{1}H NMR did not show any evidence of the peak corresponding to an N-H proton, which would have been indicative of "activation" of the terminal arylacetylene. In particular, **2a-b** remained almost unchanged upon mixing with 4-ethynylanisole for 48 h at room temperature, observing small amount of black precipitate formation for **2a**. Interestingly, when trinuclear complex **3a·[X]** was reacted with 4-ethynylanisole, complex **5a·[X]** was obtained in approximately 50% yield by ^{1}H NMR along with another undefined species. Complex **3b·[X]** also reacted with terminal arylacetylenes, however, multiple undefined products were formed, none of which resembled similar NMR pattern to **5a·[X]**, probably due to the lack of an additional pyridyl donor required for stabilization of the acetylide complex. Based on these results we can conclude that alkyne reactivity required the presence of a copper atom, since Pd-only complexes did not react. This echoes the reported accelerating "copper effect" in various types of C-C coupling reactions including the Stille, Suzuki, and Sonogashira coupling, with direct relevance for the latter.[7a-e]

Moreover, the importance of Cu···Pd distance variation was clearly observed. Comparison of the reactivity of tetra- and trinuclear Pd/Cu complexes showed that only the structures featuring short Pd···Cu contacts (ca. 2.6517(3)-2.6727(3) Å) reacted with a terminal alkyne (Scheme 3, b; type A). Such short Pd···Cu contacts are likely enabled by the coordination of

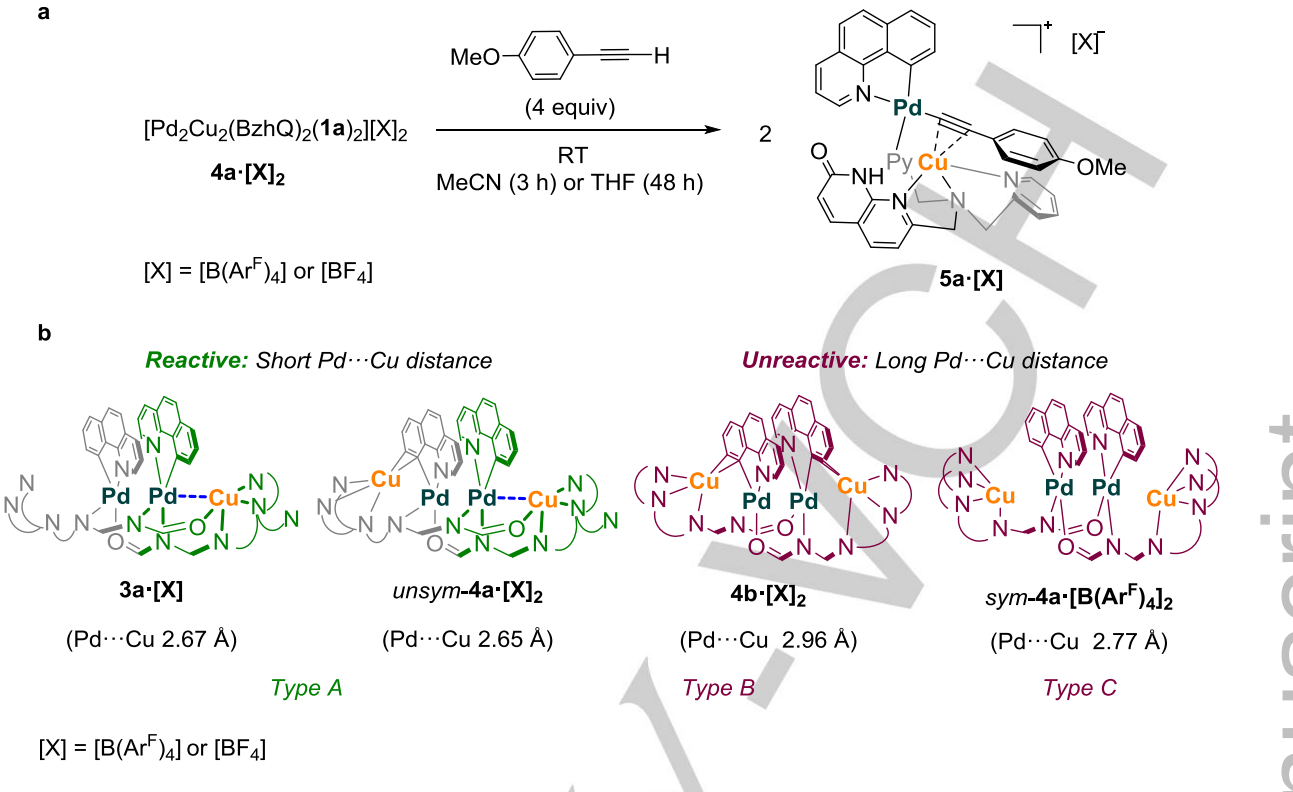

Scheme 3. (a) Reaction of complex **4a·[X]$_2$** towards 4-ethynylanisole and formation of complex **5a·[X]**. **(b)** Schematic representation of the coordination geometry around Pd···Cu core in reactive and unreactive complexes (simplified representation of ligands **1a** and **1b** is used).

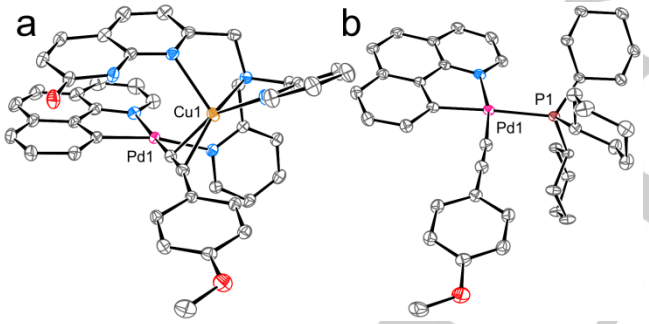

Figure 5. ORTEP of the cationic part of **5a·[B(Ar^F)$_4$]** **(a)** and compound **6** **(b)** at 50 % probability level. Counterions, hydrogen atoms, minor disordered components, and solvent molecules are omitted for clarity. The structure of **5a·[BF$_4$]** is present in the Supporting Information.

the Cu···Pd core to a rigid N,O-bridging site of naphthyridinone (Scheme 3, b; type A). Structures featuring longer Pd···Cu distances (ca. 2.8866(2)-2.9553(3) for type B and 2.7747(2)-2.8081 Å for type C) generally showed greatly diminished, or no reactivity with a terminal alkyne. Complex **4a·[B(Ar^F)$_4$]$_2$**, whose structure displayed a different coordination environment around Cu depending on the solvent (Scheme 2), also shows the same highly solvent-dependent reactivity behavior. In particular, the reaction in MeCN, where one of the major species was *unsym*-**4a·[B(Ar^F)$_4$]$_2$**, readily reacted with 4-ethynylanisole and afforded the desired product in less than 3 h at room temperature. In contrast, the same mixture in THF solution, where the major isomer is the symmetric species *sym*-**4a·[B(Ar^F)$_4$]$_2$**, required more than 72 h to complete the reaction. Although the solvent polarity effect could not be excluded, this can also be partially attributed to a much higher fraction of *unsym*-**4a·[B(Ar^F)$_4$]$_2$** with short Pd···Cu contacts. The symmetrical complex **4b·[X]$_2$** containing a Cu center with coordination to three N-donor ligands and π-interactions with benzoquinolyl, with long Pd···Cu distances, was completely unreactive under the same conditions and did not show any decomposition even upon heating.

Reductive elimination. To consider these molecular multimetallic assemblies as plausible models for Sonogashira coupling, transmetalation step should be followed by reductive elimination. Although C–C reductive elimination is commonly believed not to be a rate-limiting step in Sonogashira coupling,[6, 18] C(*sp*)-C(*sp*^{2}) reductive elimination was shown to be unfavored or even unaccessible in structural model systems studied in relation with Sonogashira coupling mechanism. As mentioned above the allyl/acetylide Pd^{II}/Cu^{I} complexes reported by Albéniz and co-workers (Figure 1, b) do not undergo C(*sp*)-C(*sp*^{2}) bond coupling even in the presence of excess of phosphine or arsine and decompose mainly via homocoupling mechanism.[9, 19] Thus, once complex **5a·[X]** bearing both aryl and acetylide groups was isolated and characterized, we carried out several experiments aiming to analyze complex **5a·[X]** reactivity in C(*sp*)-C(*sp*^{2}) bond reductive elimination in the absence or in the presence of other additives commonly used in C-C coupling reactions.

First, we tested the reactivity of complex **5a·[X]** towards C-C elimination in MeCN solution in the absence of any additive. The C-C reductive elimination step is expected to be challenging for complexes with N,O-donor ligands only that are not suitable for stabilization of the expected Pd(0) products. Expectedly, heating solutions of complex **5a·[X]** at 60-90 °C resulted in its decomposition into a mixture of unidentified products, among which no C-C coupling product was detected. Taking into account reported catalytic activity of several Pd-nitrogen containing complexes active in Cu-free Sonogashira coupling reactions,[6] we also hypothesized that detachment of the Cu^{I} ion could be required in order to induce C-C reductive elimination. We tested the stability of complex **5a·[X]**, by dissolving it in pyridine and pyridine-d_5 aiming to detach the Cu^{I} atom from the triple bond. However, under these conditions, no C(*sp*)-C(sp^2) coupling product was observed. This is consistent with limited number of examples of N-donor ligands in Sonogashira coupling.[20]

Considering that phosphines are widely known for promoting facile Sonogashira coupling,[6, 20] we then tested the reactivity of complex **5a·[X]** in the presence of various phosphine additives (PMe_3, $PhPMe_2$, PPh_3, and PCy_3). To our satisfaction, clean and selective C-C bond formation was observed in the presence of an excess of a range of commonly used phosphines, with the exception of the most bulky: PCy_3 (Scheme 6).

First, screening revealed that upon addition of 20 or more equiv of PR_3 (PR_3 = PPh_3, PMe_3, PMe_2Ph) to a MeCN solution of **5a·[X]** in MeCN at room temperature resulted in the selective formation of the desired C-C coupling product **7** (Scheme 4, a) in more than 90% yield within seconds. When complex **5a·[B(Ar^F)$_4$]** was reacted with 2.2 equiv of PMe_3 at -75 °C in THF-d_8, we also observed the formation of a reaction intermediate (**6·PMe$_3$**), which features a chemical shift of the terminal carbon bound to Pd atom at 107.2 ppm exhibiting splitting from the P-atom ($^2J_{C,P}$ = 28 Hz), which suggests that a Pd acetylide complex with one phosphine ligand in the coordination sphere was present (Figure S116).

A large excess of phosphine was required to induce C-C elimination in order to suppress a side reaction of elimination of free terminal acetylene. For example, the addition of 4 equiv of PMe_3, PPh_3 or PMe_2Ph induced the formation of 4-ethynylanisole.

Interestingly, addition of 4 equiv of PCy_3 to **5a·[X]** yields a new, mononuclear Pd aryl acetylide complex **6**, [Pd(BzhQ)(MeOPhCC)(PCy_3)] (Scheme 4, b). Complex **6** was characterized by XRD (Figure 5, b) and by NMR spectroscopy at -30 °C in CD_2Cl_2 due to its low stability at room temperature. The $^{13}C\{^1H\}$ NMR of complex **6** exhibits the characteristic signal for the C(*sp*)–Pd at 108.9 ppm and a $^2J_{C,P}$ = 23 Hz, similar to the signal observed for the intermediate **6·PMe$_3$** obtained in a reaction with PMe_3 that leads to C-C coupling (vide supra).

The isolated complex **6** does not undergo reductive elimination upon heating at 40 °C but decomposes to a mixture of unidentified products after 12 h. However, when complex **6** was combined with excess of PMe_3, immediate formation of C-C coupling product **7** was observed at room temperature. At the same time, addition of large excess of PCy_3 under analogous conditions did not result in reductive elimination, indicating the importance of the nature of the phosphine ligand used to promote the desired reductive elimination product.[3a, 3c, 21]

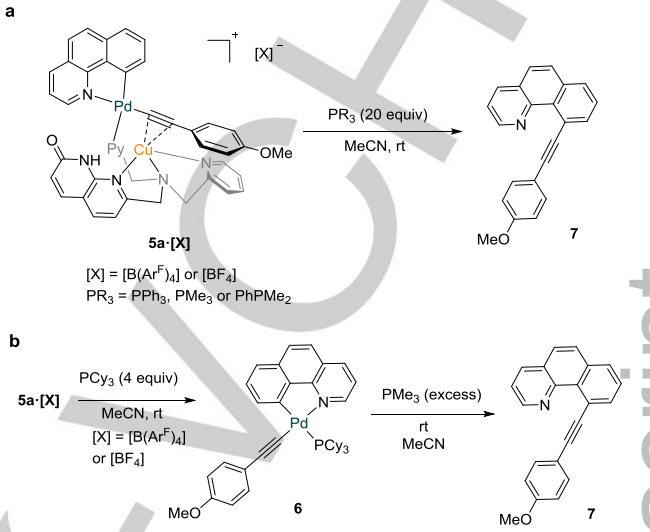

Scheme 4. C-C reductive elimination from Pd/Cu acetylide complexes. **(a)** Formation of C(*sp*)–C(sp^2) coupling product **7**. **(b)** Formation of complex **6** and C-C coupling product **7** by reaction of **6** with PMe_3.

From 4a to 5a: Mechanistic study of transmetallation. DFT calculations were performed to unravel the succession of events which occur in the alkyne activation by **4a** to give an acetylide complex **5a**. The actual experimental species (*unsym*-**4a** and ethynyl anisole) were employed in the calculations. The mechanistic investigation involved the characterization of minima and transition states via static DFT calculations (at B3LYP-D3 level optimizing in acetonitrile solvent) and investigation of large conformational changes by means of DFT-based molecular dynamics simulations combined with metadynamics to sample the Free Energy Surface (at rev-PBE-D3 level in gas phase).[16]

Initial calculations confirmed the thermodynamic feasibility of the reaction of *unsym*-**4a** with 2 equiv of 4-ethynylanisole to form 2 equiv of **5a** (Scheme 3a). The formation of the two $Pd^{II}Cu^{I}$ aryl/acetylide complexes **5a** is exergonic with a ΔG_{acn} of -5.5 kcal mol^{-1}. The Gibbs energy profile in acetonitrile for the transmetalation process leading to the formation of one molecule of **5a** from *unsym*-**4a** is depicted in Figure 6. Transition states and schematic representations of the intermediates are shown in Figures 6 and 7, respectively.

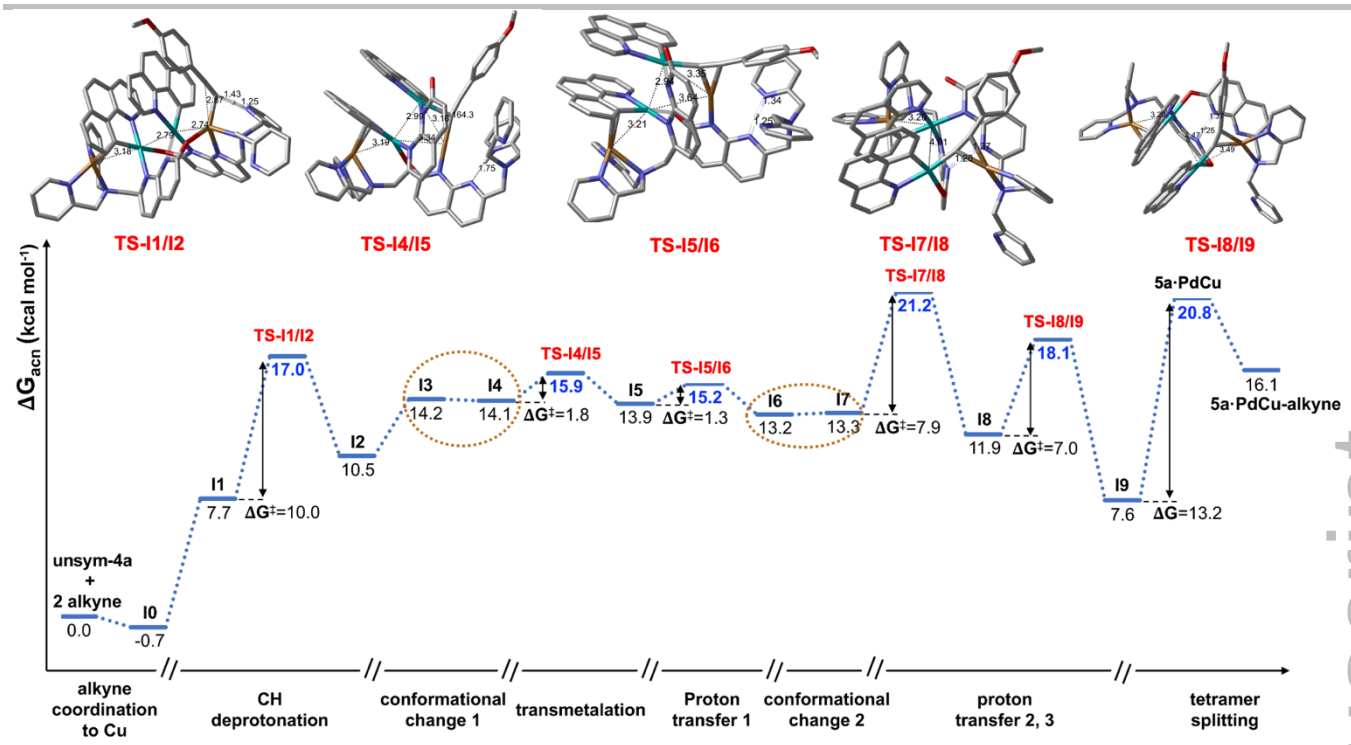

Figure 6. DFT computed (B3LYP-D3/BS2) Gibbs energy profile for formation of **5a** from *unsym*-**4a** (B3LYP-D3/BS2) in acetonitrile, ΔG_{acn}. Relative ΔG_{acn} values are given in kcal mol^{-1}. Encircled the steps analysed by metadynamics simulations.

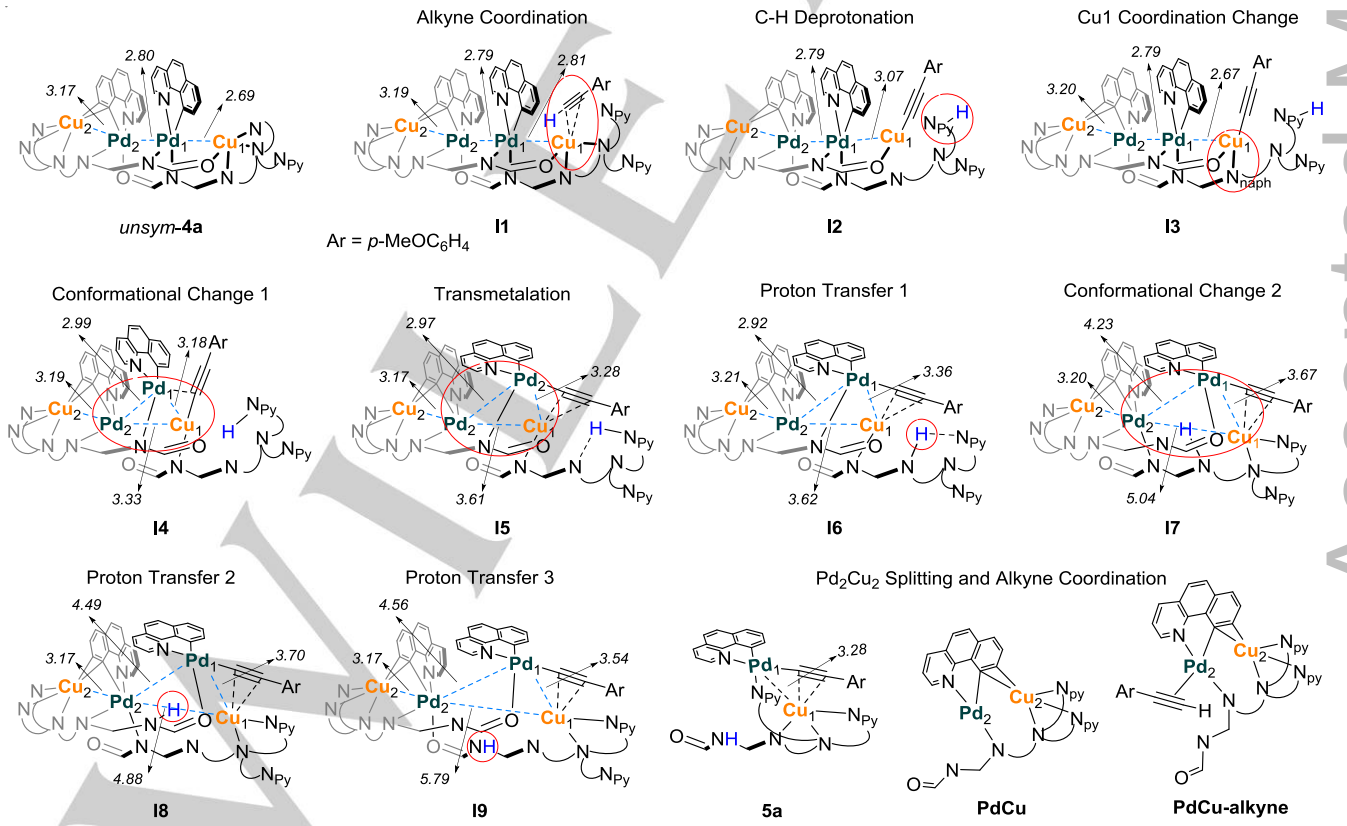

Figure 7. Schematic representation of the optimized intermediates along the pathway for the formation of **5a** from *unsym*-**4a** and 4-ethynylanisole. Intermetallic distances in Å. The titles above intermediates and red circles highlight the main rearrangements that have taken place in the step leading to the intermediate.

The process starts with the entry of the alkyne in the copper coordination sphere, initially interacting by π-π stacking with the benzoquinoline (BzhQ) aromatic ring (**I0**). Then, decoordination of one pyridyl group from the "type A" Cu^{I} (Scheme 3) allows for π-coordination of the alkyne to the Cu^{I} center (**I1**). At this point the C-H bond deprotonation takes place (**TS-I1/I2**, Figure 6) assisted by the dangling pyridyl moiety from the bis-picolyl fragment of ligand **1a**. External base is not required because the same ligand is acting as a pendant base. The computed barrier from **I0** for the CH deprotonation (17.7 kcal mol^{-1}) fits very well with the mild reaction conditions. Alkyne C-H deprotonation by other basic centers of the ligand such as the O and N atoms in Naph has higher Gibbs energy barriers (22.1 and 28.9 kcal mol^{-1}, respectively). Previous mechanistic studies of the transmetalation step in Sonogashira coupling have pointed out that transmetalation begins with π-coordination of the Pd^{II} to the Cu^{I}-acetylide fragment and proceeds to a Pd acetylide with Cu coordinated to the triple bond. [9b, 19] In **I3** the palladium atom is far away from the C≡C bond (Pd1···C1 3.65 Å; Pd1···C2 4.67 Å). Therefore, a significant structural rearrangement must happen for the palladium atom to approach this bond in **I4**. This rearrangement implies the disruption of the almost linear Cu1···Pd1···Pd2 chain in **I3** (Cu1···Pd1···Pd2 angle is 168.8° in **I3** and 65.2°in **I4**), entailing the rupture of the Pd1-N_{Naph} bond and the copper atom slipping to the nitrogen atom vacated by the Pd.

The feasibility of such reorganization has been assessed by means of *ab initio* molecular dynamics combined with metadynamics simulations (see details in the SI). With these simulations we were able to connect **I3** with **I4.** Overall, the movement that precedes transmetalation can be described as a folding of the Cu1···Pd1···Pd2 axis that allows Pd1 to be placed in front of the C≡C bond. Notably, maintaining the Cu1···Pd1 interaction along the pathway decreases its energy cost. In this respect, the unsymmetrical complex *unsym*-**4a**, displaying the shortest Pd1-Cu1distance, (XRD data: 2.6517(3) Å) is the best placed to undertake such rearrangement.

When the palladium atom reaches the π-coordination bonds of the Cu-C≡C fragment, an easy bending of the Cu-C≡C angle (**TS-I4/I5**, just 1.8 kcal mol^{-1} above **I4**, Figure 6) exchanges the σ- and π-coordinations of the two metal centers, giving intermediate **I5**, already resembling the acetylide coordination in **5a**, with the acetylide σ-coordinated to the palladium atom and π-coordinated to copper atom. The Cu1···Pd1 distance barely changes (from 3.18 Å in **I4** to 3.28 Å in **I5**) along the C-C≡C bending pathways. A secondary Pd1···Pd2 interaction maintained throughout the transmetallation process (Pd1···Pd2 distances of 2.99 and 2.97 Å in **I4** and **I5**, respectively) contributes to the stability of the system. The nature of the key σ/π coordination exchange in the actual transmetalation step is apparent from the analysis with a localized molecular orbital approach (LMOs) of the electronic rearrangements taking place in the process (Figure 8).[22]

After the acetylide transmetalation step to form σ-bonded palladium atom in intermediate **I5**, the proton transfer from the picolyl group to the nitrogen atom of the Naph ligand adjacent to the carbonyl group still needs to occur in order to obtain the final product. This nitrogen atom is also initially bonded to the copper atom in **I5**. Proton transfer from pyridyl group to the N

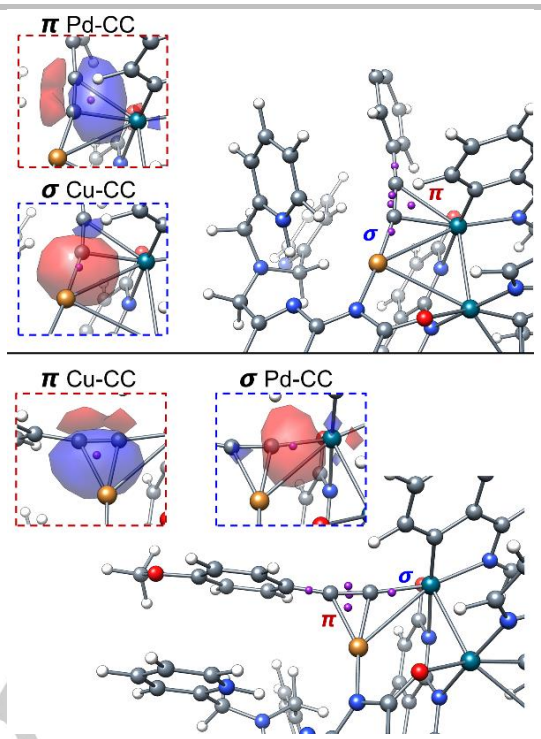

Figure 8. Analysis of the electronic rearrangements in the transmetalation step from the displacement of the center of masses of Localized Molecular Orbitals (CLMO). Top: **I4**, bottom: **I5**. Purple dots represent centroids of localized molecular orbitals.

atom of the Naph fragment takes place through a sequence of three proton-transfer steps and implies another big conformational change of the whole system. The flexible nature of the Cu1···Pd1···Pd2 chain is again invoked in order to accomplish the proton migration. In the first step, the proton is easily transferred from pyridyl moiety to the nitrogen atom in the other Naph ring (through **TS-I5/I6**, Figure 6**,** with a barrier of just 1.3 kcal mol^{-1}), yielding intermediate **I6**. Although the proton is already close to its final destination (N of Naph ring with the carbonyl substituent), it cannot be directly transferred to this nitrogen atom not only because the nitrogen lone pair is currently employed in binding Cu, but also because direct transfer would involve a high-energy four-membered ring. Instead, a rearrangement of the whole complex happens in order to place the proton in front of the equivalent nitrogen atom of the other naphthyridinone ligand (intermediate **I7**). There is a striking change in the position of the Pd2 center: while it is almost coplanar with the Cu1···C_{alkyne}···Pd1 atoms in **I6** (dihedral angle of 3°), it is placed perpendicular to this plane in **I7.** At the same time there is a slippage of the **1a** ligand bonded to Cu1, in such a way that the N-H proton is located in the vicinity of one nitrogen atom of the other Naph ring.

In order to evaluate the transformation between **I6** and **I7** intermediates, we also ran *ab initio* molecular dynamics calculations combined with metadynamics simulations, which confirm the feasibility of the **I6** to **I7** rearrangement (see SI). From **I7** the proton is transferred, with a low barrier (7.9 kcal mol^{-1}, **TS-I7/I8**, Figure 6), to the other Naph ligand (**I8**), and then with a similar barrier (7.0 kcal mol^{-1}, **TS-I8/I9**, Figure 6)

back to the first Naph ligand but at the final placement (**I9**). At this point (**I9**) the two PdCu units are held together only by the oxygen atoms of the two Naph ligands and the coordination environment at the palladium atom bearing the acetylide ligand, Pd1, is already close to that of **5a** (see optimized structures in the Supporting Information). Coordination of the dangling pyridyl moiety to Pd1 induces decoordination of oxygen, facilitating the splitting of the Pd_2Cu_2 chain into two PdCu units: **5a** and $[CuPd(BzhQ)(\mathbf{1a})]^+$ (**PdCu)**. The estimated energy cost of the dissociation of **I9** in these two units is 13.2 kcal mol^{-1} (Figure 6), suggesting that the breaking of the tetranuclear unit should occur instantaneously at room temperature during the reaction pathway. At this point, species **5a**, which contains both aryl and acetylide ligands coordinated to palladium atom in *cis*-positions is formed. The second moiety $[CuPd(BzhQ)(\mathbf{1a})]^+$ (**PdCu**) can be further stabilized by coordination of a new alkyne molecule to the Pd2 center (**5a·PdCu-alkyne**).

Calculations disclose the main features of the transmetallation process, and the way metal-metal cooperation operates in this system, that can be inferred from the analysis of the variation of Cu-Pd and Pd-Pd distances. Initially, a vacant position must be created in a copper atom to allow π-coordination of the alkyne. Alkyne coordination to a type A Cu-center (Scheme 3b) requires decoordination of only one picolyl donor, conferring higher reactivity to these centers. After π-coordination of the alkyne to Cu1 a base (the **1a** ligand in our system) deprotonates the alkyne, yielding a copper-alkynyl and implying a major change in the orientation of the C≡C bond. Then the linear Cu1···Pd1···Pd2 chain must disrupt in order for Pd1 to approach the alkynyl π-bond. The Cu1···Pd1 interaction, kept until Pd1 has coordinated the alkyne in **I4** (Cu1-Pd1 distance of 2.67 Å in **I3** and 3.18 Å in **I4**), facilitates the movement of Pd1 toward the π-bond. In this way species with initial shorter Cu···Pd distances (type A, Scheme 3b) are better suited for transmetallation. The flexibility that the ligand scaffold provides to the Pd_2Cu_2 multimetallic core is also crucial to the process, allowing the required changes in the multimetallic chain without breaking down the system. The Pd1···Pd2 interaction (Pd1···Pd2 distance between 2.80 and 2.99 Å), present until the **I6** to **I7** conformational change, also contributes to the stability of the system. The Pd2··Cu2 is almost constant all along the transformation as well as Cu2 coordination. This fact points out that Cu2 is not playing any role in the reaction, in agreement with the similar reactivity exhibited by the trinuclear complex **3a**.

Phosphine addition and C(sp^2)-C(*sp*) coupling: Mechanistic aspects. We have computationally modeled the sequential addition of two PMe_3 molecules to **5a**. The Gibbs energy profile in acetonitrile for the formation of the coupling product by adding phosphine excess to **5a** is drawn in Figure 9. Views of the structures of intermediates and transition states are shown in Figures 9 and 10. The process begins with the exchange of an N-ligand by the incoming phosphine at the palladium atom. There are two alternative pathways for this N-dissociation step, depending whether the dissociated ligand is the pyridyl arm of the picolyl fragment of **1a-H ligand** (**TS-I10/I11**), or the BzhQ ring (**TS-I10/I11'**). Both transition states have very similar energies, although the latter, **TS-I10/I11'**, is a bit lower. However, it leads to a higher energy intermediate (**I11'**). Moreover, the characterized intermediate **6** has the BzhQ ligand coordinated (Figure 5). Given the low barriers involved in this step, it appears that the reaction is under thermodynamic control and the thermodynamic product (**I11**) is formed. Dissociation of $[Cu(\mathbf{1a\text{-}H})]^+$, assisted by an additional PMe_3 molecule to form $[Cu(\mathbf{1a\text{-}H})(PMe_3)]^+$ yields the monophosphine palladium complex $[Pd(BzhQ)(MeOPhCC)(PMe_3)]$ (**6-PMe₃**), experimentally observed with PMe_3 at low temperature and characterized by X-ray with the PCy_3 variant (**6**). For further C-C coupling, the addition of a second phosphine molecule is required. This second phosphine ligand must be placed *cis* to the first one in order to allow for the reductive coupling of the aryl and acetylide ligands that are mutually *cis* as well. The difficulty of placing two bulky PCy_3 ligands *cis* to each other seems to be the reason for **6** not undergoing reductive elimination in the presence of a large excess of PCy_3.

Addition of the second PMe_3 molecule to **6-PMe₃** implies decoordination of the BzhQ ring N atom from the Pd, yielding the diphosphine intermediate $[Pd(BzhQ)(MeOPhCC)(PMe_3)_2]$ (**8**), after crossing **TS-I12/8**. This Pd^{II} diphosphine (aryl)(alkynyl) complex only requires one more transition state leading to direct reductive elimination (**TS-8/I13** yielding the coupling product **7** and $Pd(PMe_3)_2$.

10.1002/chem.202002013

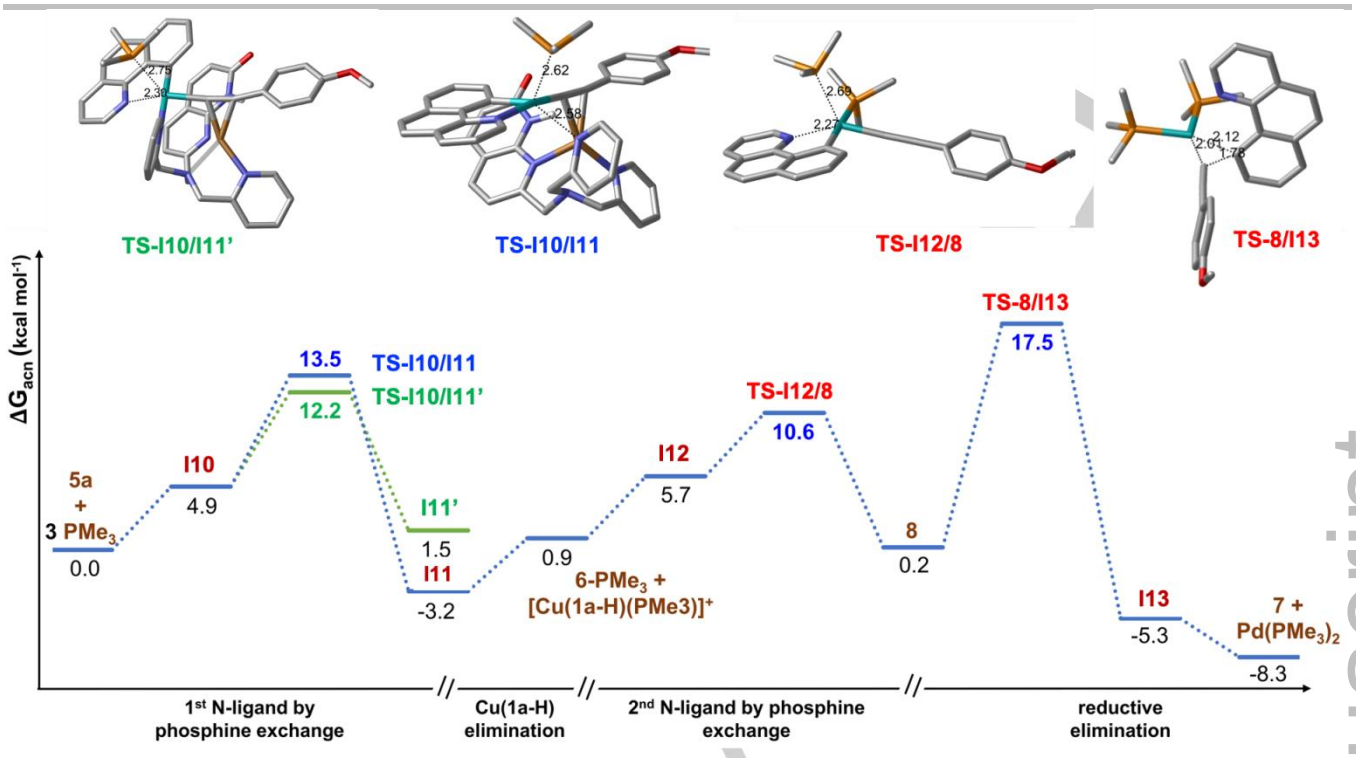

Figure 9. DFT computed (B3LYP-D3/BS2) Gibbs energy profile for the phosphine-promoted C-C coupling in acetonitrile, ΔG_{acn}. Relative ΔG_{acn} values are given in kcal mol^{-1}.

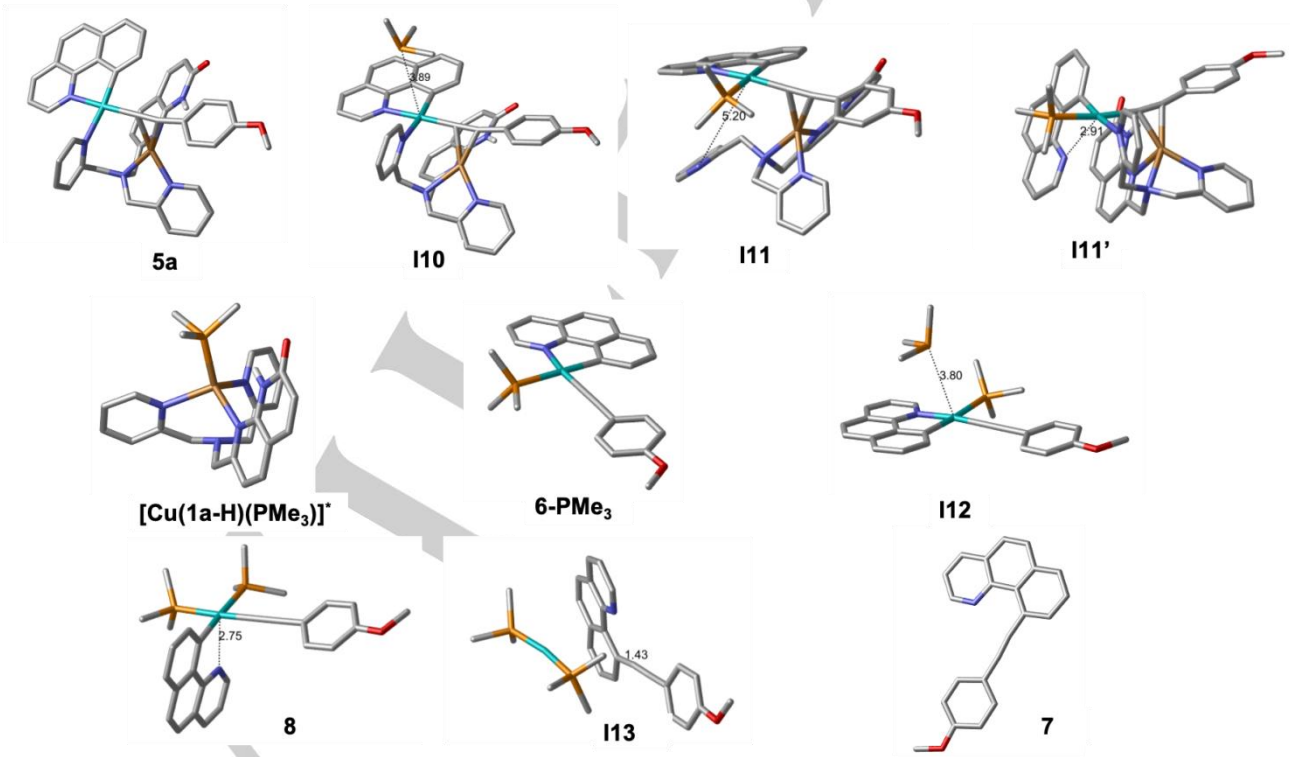

Figure 10. Optimized structures of the intermediates along the reductive elimination pathway.

Conclusion

Using dynamic polynucleating ligands, we were able to develop a general method for the selective, stepwise formation of heteromultimetallic complexes that can be used as functional models in synergistic, bimetallic catalysis. As a result, we obtained a series of organometallic Pd/Cu multimetallic complexes that serve as functional models for intermediates in Sonogashira coupling and enable a comparative study of their reactivity. We show for the first time that these functional model complexes are reactive in alkyne activation, transmetallation and C-C elimination steps. Interestingly, the N-donor ligand itself also acts as an internal base that facilitates the deprotonation of a terminal alkyne even in the absence of external base additives typically used in Sonogashira coupling. Notably, in previously studied Sonogashira model systems, these three steps had not been observed with the same complex.[9, 19] The combination of experimental and DFT studies of these systems allowed for a detailed understanding of these steps. Particularly, DFT studies highlight the importance of the dynamic behavior of the multimetallic assembly, allowing for a transmetallation from a σ-Cu/π-Pd system to form a π-Cu/σ-Pd acetylide complex with low reaction barriers. Both experimental and computational studies suggest that subtle changes in metal-metal distances and their coordination geometry have a large effect on the resulting reactivity, with the complexes featuring short Pd···Cu distances showing facile reactivity with a terminal alkyne. To conclude, these studies provide for a better understanding of the role of Pd/Cu assemblies in individual steps of Sonogashira couping and may aid in the search for new ligand designs to facilitate catalysis. Overall, such combined experimental and computational study of well-defined heteromultimetallic assemblies offers a unique tool to study metal-metal cooperation in catalysis. Considering that cyclometallated aryl Pd complexes used in this work may result from C-H bond activation, such systems also hold a potential to study multimetallic cooperation in C-H bond activation leading to the formation of C-C bonds.

Acknowledgements

We thank A. Villar-Briones and Dr. M. Roy (IAS, OIST) for HRMS analysis and acknowledge OIST for startup funding. Financial support from Spanish MINECO (A.L: CTQ2017-87889-P; A.C-V.: PGC2018-100818-A-I00 and Ramon y Cajal Fellowship RyC-2016-19930) is gratefully acknowledged. O.R.-W. was a JSPS International Research Fellow. This work was supported by JSPS KAKENHI Grant Number 16F16038.

.

Keywords: metal-metal cooperation • metal-metal interactions • Sonogashira coupling • palladium • copper

[1] a) X. Chen, K. M. Engle, D.-H. Wang, J.-Q. Yu, *Angew. Chem., Int. Ed.* **2009**, *48*, 5094-5115; b) M. Wasa, K. M. Engle, J.-Q. Yu, *Isr. J. Chem.* **2010**, *50*, 605-616; c) R. Giri, S. Thapa, A. Kafle, *Adv. Synth. Catal.* **2014**, *356*, 1395-1411.

[2] a) E. Negishi, A. de Meijere, *Handbook of Organopalladium Chemistry for Organic Synthesis*, Wiley, **2003**; b) A. de Meijere, F. Diederich, *Metal-catalyzed cross-coupling reactions*, Wiley-VCH, **2004**.

[3] a) L. Xue, Z. Lin, *Chem. Soc. Rev.* **2010**, *39*, 1692-1705; b) M. Garcia-Melchor, M. C. Pacheco, C. Najera, A. Lledos, G. Ujaque, *ACS Catal.* **2012**, *2*, 135-144; c) M. Garcia-Melchor, A. A. C. Braga, A. Lledos, G. Ujaque, F. Maseras, *Acc. Chem. Res.* **2013**, *46*, 2626-2634; d) M. Gazvoda, M. Virant, J. Kosmrlj, B. Pinter, B. Pinter, *Nat. Commun.* **2018**, *9*, 4814.

[4] a) J. He, M. Wasa, K. S. L. Chan, Q. Shao, J.-Q. Yu, *Chem. Rev.* **2017**, *117*, 8754-8786; b) P. Wang, P. Verma, G. Xia, J. Shi, J. X. Qiao, S. Tao, P. T. W. Cheng, M. A. Poss, M. E. Farmer, K.-S. Yeung, J.-Q. Yu, *Nature* **2017**, *551*, 489-493; c) Y.-F. Yang, X. Hong, J.-Q. Yu, K. N. Houk, *Acc. Chem. Res.* **2017**, *50*, 2853-2860.

[5] a) P. Buchwalter, J. Rose, P. Braunstein, *Chem. Rev.* **2015**, *115*, 28-126; b) A. E. Allen, D. W. C. MacMillan, *Chem. Sci.* **2012**, *3*, 633-658; c) M. H. Perez-Temprano, J. A. Casares, P. Espinet, *Chem. - Eur. J.* **2012**, *18*, 1864-1884; d) I. G. Powers, C. Uyeda, *ACS Catal.* **2017**, *7*, 936-958.

[6] a) R. Chinchilla, C. Najera, *Chem. Soc. Rev.* **2011**, *40*, 5084-5121; b) R. Chinchilla, C. Najera, *Chem. Rev.* **2007**, *107*, 874-922.

[7] a) L. S. Liebeskind, J. Srogl, *J. Am. Chem. Soc.* **2000**, *122*, 11260-11261; b) V. Farina, S. Kapadia, B. Krishnan, C. Wang, L. S. Liebeskind, *J. Org. Chem.* **1994**, *59*, 5905-5911; c) L. S. Liebeskind, R. W. Fengl, *J. Org. Chem.* **1990**, *55*, 5359-5364; d) P. Espinet, A. M. Echavarren, *Angew. Chem., Int. Ed.* **2004**, *43*, 4704-4734; e) J. Z. Deng, D. V. Paone, A. T. Ginnetti, H. Kurihara, S. D. Dreher, S. A. Weissman, S. R. Stauffer, C. S. Burgey, *Org. Lett.* **2009**, *11*, 345-347; f) M. Aufiero, F. Proutiere, F. Schoenebeck, *Angew. Chem., Int. Ed.* **2012**, *51*, 7226-7230.

[8] X. Wang, Y. Song, J. Qu, Y. Luo, *Organometallics* **2017**, *36*, 1042-1048.

[9] a) I. Meana, P. Espinet, A. C. Albéniz, *Organometallics* **2014**, *33*, 1-7; b) R. J. Oeschger, P. Chen, *J. Am. Chem. Soc.* **2017**, *139*, 1069-1072.

[10] O. Rivada-Wheelaghan, S. L. Aristizábal, J. López-Serrano, R. R. Fayzullin, J. R. Khusnutdinova, *Angew. Chem. Int. Ed.* **2017**, *56*, 16267-16271.

[11] D. R. Pye, N. P. Mankad, *Chem. Sci.* **2017**, *8*, 1705-1718.

[12] S. Deolka, O. Rivada, S. L. Aristizábal, R. R. Fayzullin, S. Pal, K. Nozaki, E. Khaskin, J. R. Khusnutdinova, *Chem. Sci.* **2020**, DOI 10.1039/D1030SC00646G.

[13] Deposition numbers 1890030 and 1890033-1890045 contain the supplementary crystallographic data for this paper. These data are provided free of charge by the joint Cambridge Crystallographic Data Centre and Fachinformationszentrum Karlsruhe Access Structures service www.ccdc.cam.ac.uk/structures.

[14] A. Bondi, *J. Phys. Chem.* **1964**, *68*, 441-451.

[15] B. Cordero, V. Gomez, A. E. Platero-Prats, M. Reves, J. Echeverria, E. Cremades, F. Barragan, S. Alvarez, *Dalton Trans.* **2008**, 2832-2838.

[16] See the Supporting Information.

[17] R. J. Oeschger, ETH Zurich, 2017, https://doi.org/10.3929/ethz-b-000186755.

[18] C. He, J. Ke, H. Xu, A. Lei, *Angew. Chem., Int. Ed.* **2013**, *52*, 1527-1530.

[19] R. J. Oeschger, D. H. Ringger, P. Chen, *Organometallics* **2015**, *34*, 3888-3892.

[20] J. Gil-Moltó, C. Nájera, *Eur. J. Org. Chem.* **2005**, *2005*, 4073-4081.

[21] V. P. Ananikov, D. G. Musaev, K. Morokuma, *Eur. J. Inorg. Chem.* **2007**, 5390-5399.

[22] G. Sciortino, A. Lledos, P. Vidossich, *Dalton Trans.* **2019**, *48*, 15740-15752.

10.1002/chem.202002013

Entry for the Table of Contents

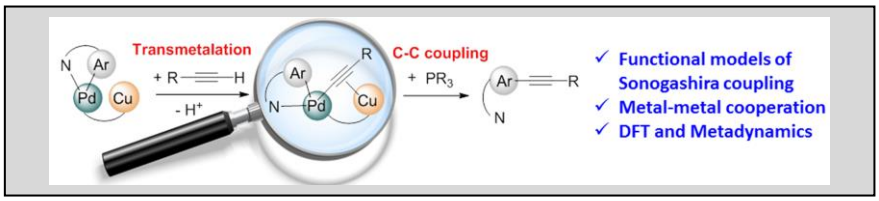

Palladium and copper synergy is investigated through the study of modular multimetallic Pd/Cu assemblies. These complexes serve as functional models of Sonogashira coupling showing reactivity in alkyne activation and C-C elimination. The effect of metal-metal distances and dynamics of multimetallic chains is elucidated through experimental and DFT studies.

Institute and/or researcher Twitter usernames: @KhusnutdinovaU @OISTedu